Device Sizing Guided by Echocardiography-Based Three-Dimensional Printing Is Associated with Superior Outcome after Percutaneous Left Atrial Appendage Occlusion

Yiting Fan, MD, Fan Yang, MD, Gary Shing-Him Cheung, MBBS, Anna Kin-Yin Chan, MBChB, Dee Dee Wang, MD, Yat-Yin Lam, MD, Marco Chun-Kit Chow, MPhil, Martin Chun-Wing Leong, MPhil, Kevin Ka-Ho Kam, MBChB, Kent Chak-Yu So, MBChB, Gary Tse, MD, Zhiqing Qiao, MD, Ben He, MD, FACC, Ka-Wai Kwok, PhD, and Alex Pui-Wai Lee, MD, FACC, *Hong Kong SAR and Shanghai, China; and Detroit, Michigan*

Background: Left atrial appendage (LAA) occlusion is an alternative to anticoagulation for stroke prevention in patients with atrial fibrillation. Accurate device sizing is crucial for optimal outcome. Patient-specific LAA models can be created using three-dimensional (3D) printing from 3D transesophageal echocardiographic (TEE) images, allowing in vitro model testing for device selection. The aims of this study were to assess the association of model-based device selection with procedural safety and efficacy and to determine if preprocedural model testing leads to superior outcomes.

Methods: In 72 patients who underwent imaging-guided LAA occlusion, 3D models of the LAA were created from 3D TEE data sets retrospectively (retrospective cohort). The optimal device determined by in vitro model testing was compared with the actual device used. Associations of model-match and model-mismatch device sizing with outcomes were analyzed. In another 32 patients, device selection was prospectively guided by 3D models in adjunct to imaging (prospective cohort). The impact of model-based sizing on outcomes was assessed by comparing the two cohorts.

Results: Patients in the retrospective cohort with model-mismatch sizing had longer procedure times, more implantation failures, more devices used per procedure, more procedural complications, more peridevice leak, more device thrombus, and higher cumulative incidence rates of ischemic stroke and cardiovascular or unexplained death ($P < .05$ for all) over 3.0 ± 2.3 years after LAA occlusion. Compared with the retrospective imaging-guided cohort, the prospective model-guided patients achieved higher implantation success and shorter procedural times ($P < .05$) without complications. Clinical device compression ($r = 0.92$) and protrusion ($r = 0.95$) agreed highly with model testing ($P < .0001$). Predictors for sizing mismatch were nonwindsock morphology (odds ratio, 4.7) and prominent LAA trabeculations (odds ratio, 7.1).

Conclusions: In patients undergoing LAA occlusion, device size selection in agreement with 3D-printed model-based sizing is associated with improved safety and efficacy. Preprocedural device sizing with 3D models in adjunct to imaging guidance may lead to superior outcomes. (J Am Soc Echocardiogr 2019;32:708-19.)

Keywords: 3D printing, Left atrial appendage occlusion, 3D transesophageal echocardiography, Structural heart intervention, Transcatheter

From the Division of Cardiology, Department of Medicine and Therapeutics, Prince of Wales Hospital, The Chinese University of Hong Kong (Y.F., G.S.-H.C., A.K.-Y.C., Y.-Y.L., K.K.-H.K., K.C.-Y.S., G.T., A.P.-W.L.), and the Department of Mechanical Engineering, The University of Hong Kong (M.C.-K.C., M.C.-W.L., K.-W.K.), Hong Kong SAR; the Division of Cardiology, Renji Hospital, Shanghai Jiaotong University, Shanghai (F.Y., Z.Q., B.H.), China; and the Center for Structural Heart Disease, Division of Cardiology, Henry Ford Health System, Detroit, Michigan (D.D.W.).

This work was funded by the Hong Kong Special Administrative Region Government Health and Medical Research Fund (05160976) and the Innovation and Technology Fund (ITS/025/16). Prof. Lee receives research equipment support from Philips Healthcare and Boston Scientific. Drs. Fan and Yang contributed equally to this work.

Conflicts of interest: None to report.

Reprint requests: Alex Pui-Wai Lee, MD, FACC, Room 114037, 9/F, Lui Che Woo Clinical Sciences Building, Prince of Wales Hospital, 30-32 Ngan Shing Road, Sha-tin, N.T., Hong Kong (E-mail: *alexpwlee@cuhk.edu.hk*).

0894-7317

https://doi.org/10.1016/j.echo.2019.02.003

Abbreviations
2D = Two-dimensional
3D = Three-dimensional
AF = Atrial fibrillation
LAA = Left atrial appendage
PASS = Position, anchor, size, seal
ROC = Receiver operating characteristic
TEE = Transesophageal echocardiographic

Among patients with nonvalvular atrial fibrillation (AF), the majority of thrombi are located within the left atrial appendage (LAA). The importance of the LAA in thromboembolic risk among patients with AF provides the rationale for occlusion of the LAA in patients who are candidates for but have either absolute or relative contraindications to long-term oral anticoagulation. Percutaneous approaches to LAA occlusion that mechanically prevent embolization of LAA thrombi have been developed and shown to be effective.[1,2] There remain, however, technical limitations in LAA occlusion that may offset its efficacy and hinder its broader application. Reportedly 1.5% to 9.1% of cases fail to achieve implantation success,[3] and serious complications, in particular pericardial effusion, are reported in 4% of procedures.[1,4] Moreover, residual peridevice leak and device thrombus have been implicated in late thromboembolic events on long-term follow-up.[5] Contributing to the challenges are the complex dimensions of the LAA and its variable morphology.[6] Optimal sizing of the LAA occluder device is a crucial factor for implantation success and may be important in maximizing the stroke-preventing efficacy of the procedure.[7] Procedural planning and device sizing are typically guided by multiplanar and/or three-dimensional (3D) transesophageal echocardiographic (TEE) imaging and fluoroscopy. However, the complexity of LAA anatomy may not be fully appreciated even with advanced imaging.[8] Failing to identify patients with LAA anatomy ineligible for device implantation can lead to implantation failure; inaccurate sizing and suboptimal positioning may lead to repeated deployment attempts that can result in procedural complications[4]; moreover, implanting a suboptimally sized device risks incomplete sealing, device migration, cardiac injury, and thrombus formation.[9]

Three-dimensional printing is a fabrication technique used to convert digital objects into physical models.[10] Three-dimensional-printed patient-specific models of the LAA can be created from 3D TEE data sets to assist in evaluating the LAA anatomy and testing the occluder device,[11] enabling more accurate sizing, particularly in complex anatomy.[12] Nevertheless, such applications have lacked the outcome analysis required to inform clinical practice. Questions remain as to whether 3D model–based device sizing can predict, and thus potentially affect, outcomes after LAA occlusion. The aims of this study were to address this and to review the relation of suboptimal LAA occluder device sizing with procedural safety and efficacy.

METHODS

Patient Population and Study Design

A total of 107 consecutive patients undergoing LAA occlusion using the WATHCMAN device (Boston Scientific, Marlborough, MA) at two academic centers (Prince of Wales Hospital and Renji Hospital) were studied. All subjects had nonvalvular AF, CHA_2DS_2-VASc scores ≥ 1, and relative or absolute contraindications to long-term anticoagulation. This study is a mix of retrospective and prospective analysis. In 74 early patients, LAA occlusion was guided by imaging alone with 3D transesophageal echocardiography and fluoroscopy. The 3D TEE images in these patients were processed retrospectively for 3D printing of the LAA. In two patients, 3D TEE image quality was not sufficient for the creation of a 3D model. The remaining 72 patients with adequate 3D TEE images constituted the retrospective cohort of this study. The subsequent 33 patients were studied prospectively, with 3D printing of LAA models performed before the clinical occlusion procedures. The quality of 3D TEE images was adequate for 3D printing in all prospective patients. Of these 33 patients, one patient was eventually excluded from LAA occlusion because the original 3D TEE data suggested that LAA depth was insufficient for device implantation, with confirmation by in vitro model testing. The remaining 32 patients constituted the prospective 3D printing cohort of this study.

The retrospective group served as the derivation cohort, on the basis of which the model-based sizing method was established. The cutoff defining match or mismatch with the models derived from the retrospective cohort (see "Statistical Analysis") was tested in the prospective group. The two cohorts also represented different strategies for device selection, with the retrospective cohort using an imaging-only (transesophageal echocardiography and fluoroscopy) sizing strategy and the prospective cohort a model-based strategy. The study protocol was approved by the local institutional review board.

Echocardiography and 3D Printing

Three-dimensional TEE imaging is considered the standard of care for preprocedural planning and procedural guidance of LAA occlusions at our centers.[7] Three-dimensional TEE imaging was performed using an iE33 or EPIQ7C ultrasound system (Philips Medical Systems, Andover, MA) equipped with a fully sampled matrix transducer (X7-2t). During both preprocedural and procedural TEE imaging, 3D data sets of the LAA were acquired using "3D zoom" mode at the midesophageal level, encompassing the appendage, left pulmonary vein ridge, and part of the left atrium,[13] maximizing blood-tissue contrast, especially the appendicular trabeculations (Figure 1). Images in end-systole were exported in Cartesian Digital Imaging and Communications in Medicine format for segmentation (Mimics 19.0; Materialise, Leuven, Belgium). After filtering for noise, blood volume of the LAA was segmented semiautomatically by threshold pixel intensity. A geometric surface mesh model was generated and refined to create a hollow cast with 1-mm wall thickness, on the basis of the mean atrial wall thickness previously reported.[14] The digital model was exported as stereolithography files for 3D printing in a 1:1 scale on a high-resolution (32 μm) PolyJet 3D printer (Objet350 Connex3; Stratasys, Eden Prairie, MN). A rubber-like (30–35 scale A shore hardness), tear-resistant (5–7 kg/cm), translucent photopolymer material (Agilus30 Clear; Stratasys) with tensile properties (2.4–3.1 MPa) mimicking cardiovascular tissue was used for printing. Three-dimensional printing for retrospective subjects used preprocedural 3D transesophageal echocardiography as the image source unless a more than ± 1 mm pre- or intraprocedural discrepancy of measured LAA ostial diameters and/or depth existed, in which case we used the intraprocedural preimplantation 3D TEE images after left atrial pressure was raised to ≥ 10 mm Hg, which was performed in all patients. For later patients with prospective 3D modeling, we routinely administered a 500- to 1,000-mL intravenous bolus of normal saline before preprocedural TEE imaging to ensure adequate loading.[15] The major and minor ostial diameters and depth of 3D models were measured using a digital caliper.

HIGHLIGHTS

- Three-dimensional printing of LAA models on the basis of 3D TEE images is feasible.
- LAA device compression and position in models correlate with actual procedure.
- Patients with implanted device matching model testing have better procedural outcomes.
- 3D printing guidance for LAA occlusion may lead to improved outcomes.

Occluder Device Sizing

For the retrospective cohort, in vitro device implantation was performed within the 3D models by two independent investigators (Y.F. and A.P.-W.L.) blinded to the results of the clinical procedure for determination of the optimal device size. The full range of WATCHMAN occluder device sizes (21–33 mm) was tested in the models with different implantation depths through a commercial delivery system. The delivery catheter was positioned in the distal lobes of the models before device deployment, maintaining coaxiality similar to a standard clinical procedure. In vitro device compression and protrusion in the models were measured using a digital caliper. Device compression was defined as the percentage reduction of the device maximal diameter measured at the device "shoulders."[9] The PASS (position, anchor, size, seal) device release criteria were assessed in the 3D models: (1) position at or just distal to ostium with protrusion < 40% to 50% device depth, (2) all anchors engaged with stable tug test, (3) device shoulder compressed 8% to 20% or up to 30% if results otherwise optimal, and (4) adequate seal with residual leak or gap ≤ 5 mm (Figure 1). Model testing started with the device size predicted by TEE imaging, and if the PASS criteria were not met, the next larger or smaller size was tested. The device size that best fulfilled all four PASS criteria was considered the optimal device for LAA occlusion. Reproducibility of model-based device sizing and measurements of device compression and protrusion within models was determined by repeating in vitro model testing ≥1 week after the initial test by the same observer (intraobserver) and a different observer (interobserver) in 15 randomly selected cases.

For the prospective patients, two experienced interventional operators (G.S.-H.C. and B.H.) performed the in vitro model testing as an adjunct to 3D TEE imaging and fluoroscopy for guiding device selection before they performed the clinical implantation of the device.

The occluder device was implanted using a transfemoral transseptal approach.[9] The transseptal puncture was guided using matrix-array biplane (xPlane) mode in the bicaval (~90°) and short-axis (~45°) views to achieve an inferoposterior puncture location. Intraprocedural two-dimensional (2D) TEE measurement of the LAA was performed after raising LA pressure to ≥10 mm Hg with intravenous normal saline, with the major and minor ostial diameters (measured from the circumflex artery inferiorly to a point superiorly 1–2 cm within the pulmonary vein ridge) and depth (from ostium to LAA apex) recorded by sweeping through the standard imaging planes from 0° to 135°.[7,9,13] The major and minor ostial diameters and depth were also measured on multiplanes reconstructed on-cart from the native 3D TEE imaging data acquired using 3D zoom mode[13] and made available to the operators. Device sizing at the time of implantation was made at the operator's discretion, using data from all available modalities (2D and 3D TEE imaging, fluoroscopy, and 3D modeling), with 3D TEE measurements used preferentially over 2D measurements for sizing in the retrospective cohort, as previously reported,[7,13] and with preprocedural 3D model–based sizing in the prospective cohort. After crossing the interatrial septum, the delivery catheter was advanced over a pigtail deep into the distal anterior lobes of the LAA, ensuring coaxiality between the catheter and the LAA body before and during device deployment under simultaneous biplane (~45° and 135°) imaging. Implantation success was defined as successful device release after fulfillment of four PASS criteria upon systematic assessment on multiplanar TEE imaging and fluoroscopy (Figure 1).[1-3]

Follow-Up

After LAA occluder implantation, patients were treated with oral anticoagulation (warfarin or a direct oral anticoagulant) and aspirin for 1 to 3 months, followed by TEE imaging. If TEE imaging showed residual leak ≤5 mm and no device thrombus, anticoagulation was switched to dual-antiplatelet therapy until 6 months after implantation, followed by aspirin indefinitely. Patients deemed absolutely contraindicated for anticoagulation were treated with dual-antiplatelet therapy for 6 months after implantation. If significant leak (>5 mm) and/or thrombus was detected on follow-up TEE imaging, anticoagulation continued until resolution of the leak or thrombus or indefinitely at the physician's discretion. Follow-up visits occurred at 1, 3, 6, and 12 months and twice a year thereafter. Standardized definition of outcome events was used as previously reported.[1-4] Procedure-related safety events were defined as events happening within 7 days of the procedure.[4] Pericardial effusions were considered serious either if they were of hemodynamic significance prompting intervention or if they extended hospitalization.[4] The composite end point for long-term efficacy consisted of the occurrence of all stroke (ischemic and hemorrhagic), systemic embolism, and cardiovascular or unexplained death.[1]

Statistical Analysis

Data are expressed as mean ± SD, median, range, or counts and percentages. Data normality was analyzed using the Shapiro-Wilk test. For the retrospective cohort, a receiver operating characteristic (ROC) curve was generated using adverse outcome as the end point (state variable). Adverse outcome was defined as the occurrence of any of the following: implantation failure, any procedural safety event within 7 days, significant peridevice leak (>5 mm), device thrombus, or composite efficacy events including all stroke, systemic embolism, or cardiovascular or unexplained death. Areas under the curve were evaluated for model-based device sizing, using the absolute Δ (absolute value of [diameter of device fulfilling PASS criteria in model] minus [diameter of device clinically used for initial implant]) as the independent variable. Specific upper cutoff for model-device match or mismatch was defined using the ROC curve, on the basis of the absolute Δ corresponding to the highest sum of the sensitivity and specificity for discriminating adverse and nonadverse outcomes. The cutoff thus derived was used to classify patients as "model match" or "model mismatch." The associations of model match or mismatch with outcomes were analyzed in the retrospective cohort. The impact of the preprocedural model-based device sizing strategy on procedural outcomes was assessed by comparing event rates between the retrospective (imaging-only sizing) and prospective (model-based sizing) cohorts. Group

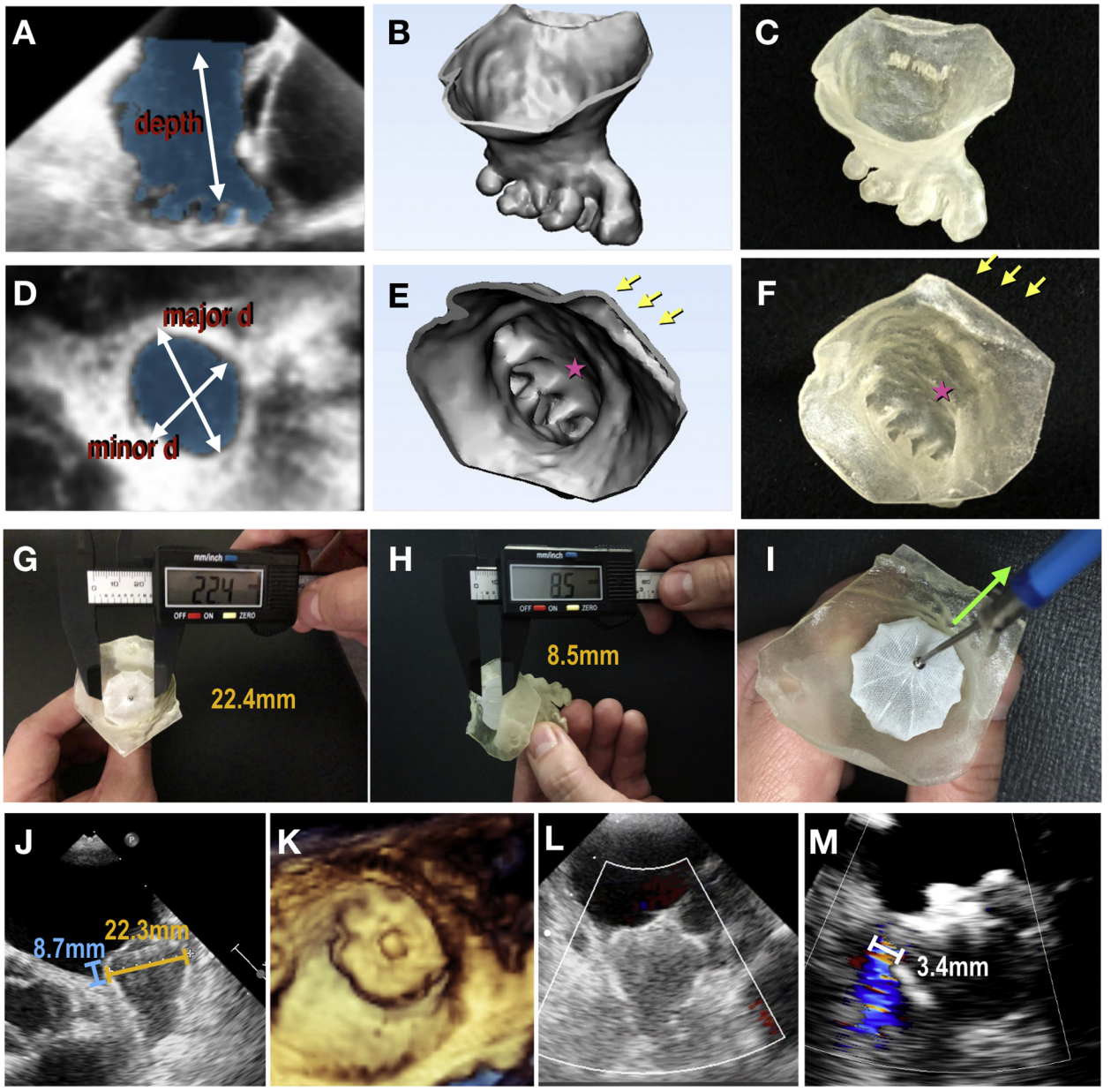

Figure 1 Echocardiography-based 3D printing of patient-specific models. **(A–F)** From 3D TEE image to 3D physical model. **(A, D)** Segmentation of LAA (*shaded area*) on 3D TEE data. The major and minor ostial diameters and depth of the LAA are measured. **(B, E)** Digital object created. **(C, F)** Three-dimensional-printed physical model made of tissue-mimicking material. **(A–C)** Long-axis views and **(D–F)** short-axis views demonstrating oval shape of the ostium. *Arrows* denote pulmonary vein ridge; *stars* denote appendicular trabeculations. **(G–I)** Device sizing in 3D model. **(G)** Device compression and **(H)** protrusion in 3D model measured using a digital caliper. Note the device-related deformation of the 3D-printed models, with the oval ostium becoming rounded after the deployment of a round WATCHMAN device. **(I)** Tug test for stability (Video 1; available at www.onlinejase.com). **(J)** Device compression and protrusion measured in clinical procedure. **(K)** Three-dimensional TEE en face view of final device position. **(L)** Color Doppler assessment showing no peridevice leak. **(M)** In another case, color Doppler assessment revealed residual leak with a jet width of 3.4 mm.

comparisons of outcome used Student's *t* test, the Wilcoxon test, or the Fisher exact test as appropriate. Time-related events were analyzed using Kaplan-Meier curves. The effect of sizing mismatch with the 3D model, baseline patient characteristics, and procedural variables on long-term efficacy of LAA occlusion was assessed using Cox proportional-hazard models. Agreement between 3D model and TEE measurements and that between in vitro and in vivo device compression and protrusion were assessed with Pearson coefficient and Bland-Altman method. Intra- and interobserver variability of continuous measurements of in vitro device compression and protrusion was assessed using intraclass correlation coefficients and the Bland-Altman method. Intra- and interrater agreement of model-based sizing was assessed using κ statistics. Predictors of model-mismatch sizing were explored. Analyses were performed using JMP version 12.0 (SAS Institute, Cary, NC). P values $< .05$ were considered to indicate statistical significance.

Table 1 Baseline characteristics

Variable	Retrospective cohort (n = 72)	Prospective cohort (n = 32)	P*	Total (N = 104)
Age (y)	73 ± 8	71 ± 8	.24	72 ± 8
Men	46 (63.9)	20 (62.5)	.89	66 (63.5)
Type of AF			.71	
Paroxysmal	20 (30.6)	12 (37.5)		34 (32.7)
Persistent	10 (13.9)	5 (15.6)		15 (14.4)
Permanent	40 (55.6)	15 (46.9)		55 (52.9)
CHA_2DS_2-VASc score	4.3 ± 1.4	3.7 ± 1.7	.08	4.1 ± 1.5
Coronary heart disease	28 (38.9)	17 (53.1)	.18	45 (43.3)
Diabetes	36 (50.0)	12 (37.5)	.24	48 (46.2)
Hypertension	55 (76.4)	22 (68.8)	.41	77 (74.0)
Heart failure	18 (25.0)	5 (15.6)	.29	23 (22.1)
Prior ischemic stroke/TIA	28 (38.9)	7 (21.9)	.09	35 (33.7)
Chronic kidney disease	11 (15.3)	2 (6.3)	.20	13 (12.5)
LAA anatomy				
Maximal ostial diameter (mm)	24.4 ± 3.3	23.9 ± 2.9	.40	24.3 ± 3.2
Minimal ostial diameter (mm)	19.4 ± 3.9	19.1 ± 3.2	.69	19.3 ± 3.6
Depth (mm)	33.3 ± 4.5	33.9 ± 5.2	.57	33.5 ± 4.7
Number of lobes	2 (1–4)	2 (1–3)	.79	2 (1–4)
Morphology			.79	
Chicken wing	12 (16.7)	4 (12.5)		16 (15.4)
Windsock	18 (25.0)	10 (31.3)		28 (26.9)
Cauliflower	23 (31.9)	11 (34.4)		34 (32.7)
Cactus	19 (26.4)	7 (21.9)		26 (25.0)
Initially selected device			.86	
21 mm	2 (2.8)	0 (0)		2 (1.9)
24 mm	19 (26.4)	7 (21.9)		26 (25.0)
27 mm	26 (36.1)	12 (37.5)		38 (36.5)
30 mm	15 (20.8)	8 (25.0)		23 (22.1)
33 mm	10 (13.9)	5 (15.6)		15 (14.4)
Implanted device			.84	
21 mm	2 (2.8)	1 (3.1)		3 (2.9)
24 mm	13 (18.1)	6 (18.8)		19 (18.3)
27 mm	28 (38.9)	12 (37.5)		40 (38.5)
30 mm	16 (22.2)	8 (25.0)		24 (23.1)
33 mm	9 (12.5)	5 (15.6)		14 (13.5)
None (implantation failure)	4 (5.6)	0 (0)		4 (3.8)
Post-LAA occlusion antithrombotic regimen			.38	
Warfarin	38 (52.8)	15 (46.9)		53 (51.0)
DOAC	10 (13.9)	8 (25.0)		18 (17.3)
DAPT	24 (33.3)	9 (28.1)		33 (31.7)

DAPT, Dual-antiplatelet therapy; *DOAC*, direct oral anticoagulant; *TIA*, transient ischemic attack.
Data are expressed as mean ± SD, number (percentage), or median (range).
*Retrospective versus prospective cohort.

RESULTS

Study Population

Baseline characteristics of the retrospective and prospective cohorts are shown in Table 1. There were no differences in demographic, clinical, and procedural characteristics between the two cohorts.

ROC Curve Analyses for Defining Device Match and Mismatch with Model-Based Sizing

The ROC curve analysis showed that in vitro model testing had good discriminatory value for adverse outcomes, with an area under the curve of 0.81 (P = .0002; see Supplemental Figure 1 in the

Table 2 Device sizing mismatch with 3D model and procedural events within 7 days in the retrospective cohort

Variable	Model-match group	Model-mismatch group	*P*
Procedural performance			
Procedure time (min), median (range)	50 (25–150)	60 (35–150)	.03
Implantation success	52/52 (100.0)	15/20 (75.0)	.0011
Devices used per procedure, mean (range)	1.1 (1–3)	1.7 (1–4)	<.0001
Device resizing	0/52 (0.0)	9/20 (45.0)	<.0001
Deployment attempts per procedure, mean (range)	1.6 (1–5)	3.0 (1–5)	<.0001
Major procedural adverse safety events within 7 days			
Death	0/52 (0.0)	0/20 (0.0)	NA
Stroke/TIA	0/52 (0.0)	0/20 (0.0)	NA
Serious pericardial effusion	1/52 (1.9)	4/20 (20.0)	.019
Pericardial tamponade	1/52 (1.9)	3/20 (15.0)	.03
Pericardial effusion, no intervention	0/52 (0.0)	1/20 (5.0)	.28
Device embolization	0/52 (0.0)	0/20 (0.0)	NA
Air embolism	1/52 (1.9)	0/20 (0.0)	≥.999
Major bleed	0/52 (0.0)	0/20 (0.0)	NA
Composite procedural major safety events within 7 days	2/52 (3.9)	4/20 (20.0)	.047
Other procedural events			
Minor bleed (hematoma)	0 (0.0)	1 (5.0)	.28

NA, Not applicable; *TIA*, transient ischemic attack.
Data are expressed as number/total (percentage) except as indicated.

Appendix, available at www.onlinejase.com). An upper cutoff of absolute Δ 3 mm had sensitivity of 73% and specificity of 84%. Because each available size (21, 24, 27, 30, and 33 mm) of the WATHCMAN LAA occluder differs by 3 mm, patients were classified as "model match" if the first device used in the clinical procedure was the same (i.e., less than one size difference) as that determined by in vitro model testing; otherwise they were classified as "model mismatch."

Model-Mismatch Sizing and Procedural Safety in the Retrospective Cohort

In the retrospective cohort, the device used in the clinical procedure matched the model-based sizing in 52 of 72 patients (model-match group) and did not match in 20 of 72 (model-mismatch group). Table 2 compares procedural performance and adverse safety events within 7 days in the model-match and model-mismatch groups in the retrospective cohort. The overall implantation success rate in the retrospective cohort was 93.1% (67 of 72). All patients with model-match device sizing achieved implantation success without the need for resizing. In contrast, patients with model-mismatch sizing experienced longer procedure time, more deployment attempts, device resizing, implantation failures, and procedure-related complications within 7 days, driven by more serious pericardial effusion ($P < .05$ for all).

All serious effusions occurred during or within 24 hours of the procedure. Of the five effusions, four required intervention and one did not require intervention but extended the patient's hospital stay by 2 days. On the basis of a review of procedural details, fluoroscopy and TEE imaging, and surgical findings, a root-cause analysis of effusions was performed (Table 3). LAA injury was surgically implicated in three of the five effusions. In two of these three cases, 3D modeling suggested that the devices used were too large, which might have caused the LAA injury (Figure 2A–F). In the remaining case, a 27-mm device was initially used but failed to achieve adequate occlusion with a leak up to 5 mm despite two deployment attempts; a 30-mm device was exchanged, with two failed attempts to cover a proximal lobe, achieving adequate seal only on the third attempt. Pericardial tamponade developed after device release. Three-dimensional modeling predicted that the 27-mm device was too small and that the 30-mm device should have been used initially and deployed proximally. In the one effusion not requiring intervention, the largest ostial diameter measured 29 mm on 3D TEE imaging; a 33-mm device was deployed but extruded by prominent trabeculations near the landing zone despite four repeated attempts; implantation failed and effusion developed within 8 hours. In this case, 3D modeling showed that no available WATCHMAN device could achieve stable anchoring, because of the presence of prominent trabeculation near the landing zone. Multiple device deployments (four or five times) in the above two cases might have contributed to the effusions. In the remaining case, a 33-mm device was implanted successfully with a single attempt, but effusion developed before LAA entrance of the delivery system. This effusion was purportedly unrelated to device sizing.

Model-Mismatch Sizing and Device Complications in the Retrospective Cohort

Follow-up TEE imaging was performed in 64 of 72 patients in the retrospective cohort 56 ± 17 days after LAA occlusion. TEE imaging was not performed in eight patients, because of failure to implant ($n = 4$), death before follow-up TEE imaging ($n = 2$), surgical ligation of the LAA after pericardial effusion ($n = 1$), and patient refusal ($n = 1$). Table 4 compares the follow-up TEE findings in the model-match and model-mismatch groups. The model-mismatch group had greater peridevice leak and more device thrombus ($P < .05$). Four thrombi were identified on device surface at a median of

Table 3 Cause analysis of procedural complications

Patient	Complication	Morphology of LAA	Size based on 3D model (mm)	Size of first device implanted (mm)	Size of final device implanted (mm)	Sizing mismatch with 3D model	Number of deployment attempts	Surgical findings	Possible cause(s)
1	Tamponade with surgical intervention	Chicken wing	30	27	30	+	5	• Hemopericardium • Fibrin clot over left atrium	• Multiple deployments
2	Tamponade with surgical intervention	Cauliflower	24	27	27	+	2	• Hemopericardium • Bruises over LAA	• Multiple deployments • Oversized device
3	Tamponade with surgical intervention	Cactus	21	24	24	+	1	• Bleeding sites from LAA	• Oversized device • Delivery sheath manipulation
4	Pericardial effusion, no intervention	Cactus, prominent trabeculations	Ineligible for WATCHMAN	33	None	+	4	N/A	• Multiple device deployments
5	Tamponade with percutaneous drainage	Windsock	33	33	33	–	1	N/A	• No definitive cause identified • Pulmonary vein injury
6	Coronary air embolism with transient ST-segment elevation	Cactus	30	30	30	–	1	NA	• Air seen in left-sided circulation by echocardiography

NA, Not applicable.

87 days (range, 55–212 days) after LAA occlusion. All thrombi were associated with peridevice leaks, with jet width ranging from 3.3 to 6.9 mm; three of the four thrombi were located in a cul-de-sac formed between the device and prominent left pulmonary vein ridge; two of these three patients sustained ischemic stroke 208 and 264 days after LAA occlusion (discussed later). In these three cases, in vitro model testing suggested that larger devices should have been used to avoid deep implantation (Figure 3).

Model-Mismatch Sizing and Long-Term Outcomes in the Retrospective Cohort

Over a mean follow-up duration of 3.0 ± 2.3 years, there were two ischemic strokes (as mentioned earlier), one hemorrhagic stroke, three cardiovascular or unexplained deaths, and six noncardiovascular deaths in the retrospective cohort (Table 5). Patients with model-mismatch device sizing had markedly lower survival free from the composite efficacy end point (log-rank $P = .0009$), ischemic stroke (log-rank $P = .01$), and cardiovascular or unexplained death (log-rank $P = .039$) compared with patients with model-match sizing (Figure 4). Comparing patients with and without composite efficacy events, there were no differences in age, sex, type of AF, coronary heart disease, diabetes, hypertension, prior ischemic stroke or transient ischemic attack, and post–LAA occlusion antithrombotic regimen ($P > .50$ for all). Patients with composite efficacy events had higher baseline CHA_2DS_2-VASc score (5.4 ± 0.5 vs 4.2 ± 1.5, $P = .003$), prevalence of prior heart failure (four of five vs 14 of 67, $P = .01$), and chronic kidney disease (three of five vs eight of 67, $P = .02$). After adjusting for CHA_2DS_2-VASc score and comorbidities, model-mismatch device sizing was associated with a 16.3-fold increase in the risk for composite efficacy events (adjusted hazard ratio, 16.3; 95% CI, 1.8–148.0; $P = .01$). Of the two cardiovascular or unexplained deaths in the model-mismatch group, one patient was implanted with an undersized device by 3D model sizing with significant residual leak (6 mm) and died suddenly at home 1.5 years after LAA occlusion after stopping oral anticoagulation (Figure 2G–J); another patient died of heart failure 5 years after LAA occlusion.

Preprocedural 3D Model–Based Device Sizing in the Prospective Cohort

There were no discrepancies between the pre- and intraprocedural 3D TEE measurements of the ostial major and minor diameters and depth ($P > .10$ for all). In the prospective cohort, 3D model–based prediction of device size agreed with the finally implanted device in 31 of 32 cases (96.9%). Implantation success was 100%. Table 6 compares the procedural outcomes and follow-up TEE device status between the imaging-guided retrospective cohort and the model-guided prospective cohort. Compared with the retrospective cohort, the prospective patients achieved higher implantation success rate, shorter procedural time, fewer devices used per procedure ($P < .05$ for all), and no procedural complications. Follow-up TEE imaging showed no residual leak in all but one case, for which the interventional operator implanted at his discretion a device smaller than that suggested by 3D model testing; in this case, follow-up TEE imaging showed a residual 3 mm peridevice leak. Over a mean follow-up duration of 9.4 ± 4.1 months, there were no mortality, stroke, or other major adverse events in the prospective cohort. Three-dimensional TEE device size suggestions were concordant with final device sizes in 18 patients (56.3%), while 13 cases (40.6%) would have been undersized and one case

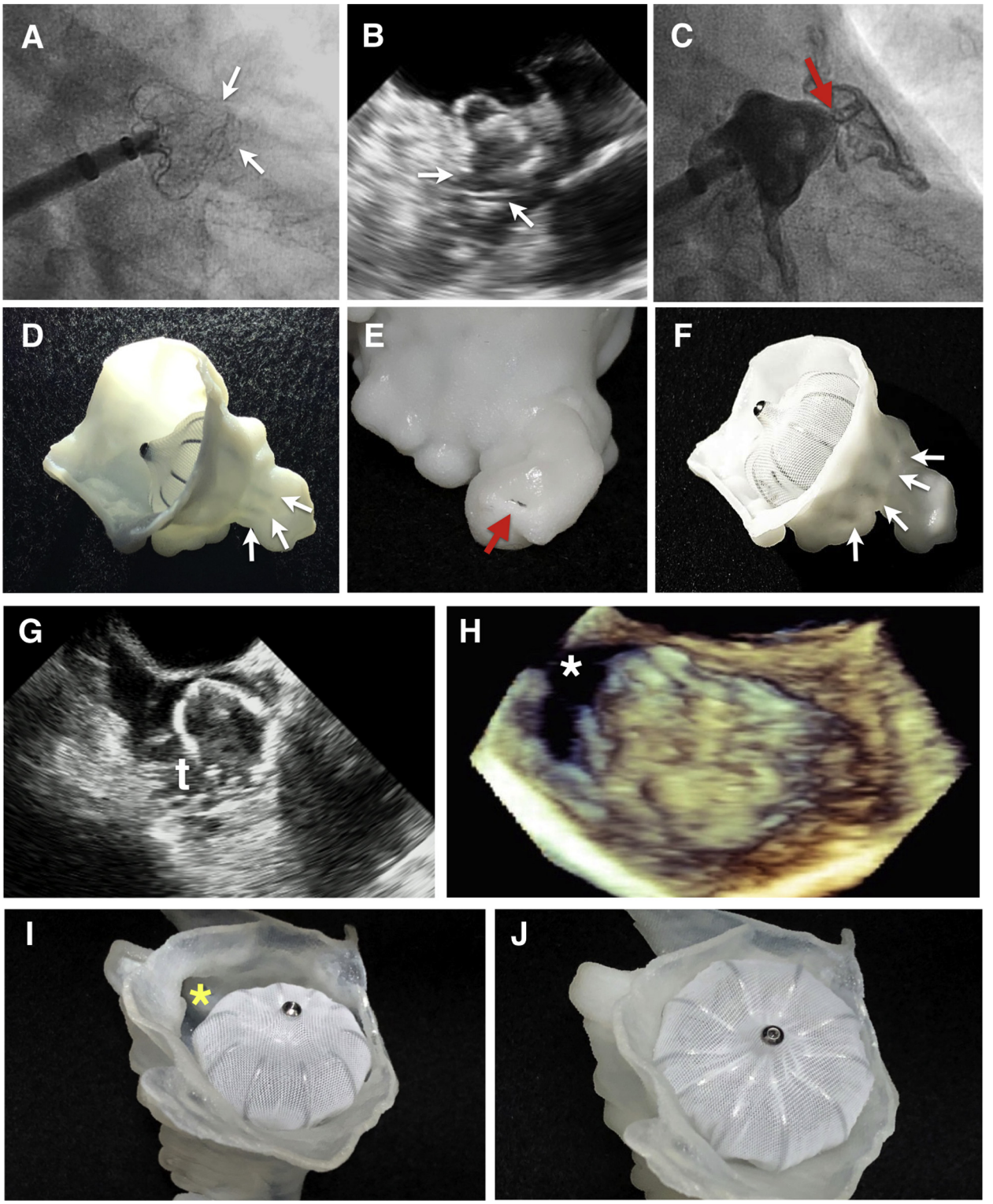

Figure 2 Cases with implantation failure and pericardial tamponade. Case 1: A 24-mm device deployed in a cactus-shaped LAA with a tapering apex failed to fully retract (*white arrows*) on fluoroscopy **(A)** and TEE imaging **(B)**. Immediately after deployment, tamponade developed, and **(C)** angiography showed contrast extravasation (*red arrow*) through the LAA apex into the pericardial space. **(D)** Three-dimensional model shows that the 24-mm device was too large to retract into an anchored configuration with the unretracted fixation barbs (*white arrows*) exerting localized pressure. **(E)** A small perforation (*red arrow*) is seen near the apex of the LAA model. **(F)** Deployment of a 21-mm device would have resulted in proper retraction of the fixation barbs (*white arrows*). Case 2: **(G)** Prominent LAA trabeculations (t) interfered with device deployment. **(H)** A 27-mm device chosen on the basis of 3D TEE measurements did not achieve adequate LAA occlusion of the oval-shaped orifice, with significant (6-mm) peridevice leak (*white asterisk*). **(I)** The 3D model accurately reveals the leak (*yellow asterisk*). This patient died suddenly 1.5 years after LAA occlusion. **(J)** A 33-mm device would have achieved adequate occlusion.

Table 4 Device sizing mismatch with 3D model and follow-up TEE device complications in the retrospective cohort*

Variable	Model-match group	Model-mismatch group	*P*
Device thrombus	1/51 (2.0)	3/13 (23.1)	.02
Peridevice leak			.008
None	33/51 (64.7)	8/13 (61.5)	
<1 mm	1/51 (2.0)	0/13 (0)	
1–3 mm	16/51 (31.4)	1/13 (7.7)	
>3–5 mm	1/51 (2.0)	3/13 (23.1)	
>5 mm	0/51 (0)	1/13 (7.7)	
Jet width in subjects with leak (mm)	2.2 (0.8–4.9)	4.3 (2.5–6.9)	.005

Data are expressed as number/total (percentage) or as mean (range).
*Assessed in 64 of 72 patients in the retrospective cohort with follow-up TEE imaging performed (see text for details).

(3.1%) would have been oversized by 3D TEE imaging. Two-dimensional TEE size suggestions were concordant with the finally implanted sizes in only 13 cases (40.6%); for the remaining 19 cases (59.3%), 2D TEE device sizing was too small.

Reproducibility of In Vitro Model Testing and Correlation with In Vivo Measurements

Measurement reproducibility (intraclass correlation coefficient, bias, and limits of agreement) for intraobserver variability of in vitro device compression and protrusion measurements was as follows: compression, 0.94, 0.01%, and −0.04% to 0.06%; and protrusion, 0.95, 0.49%, and −2.4% to 3.4%. Measurement reproducibility (intraclass correlation coefficient, bias, and limits of agreement) for interobserver variability of in vitro device compression and protrusion measurements was as follows: compression, 0.89, 0.02%, and −0.05% to 0.09%; and protrusion, 0.94, 0.5%, and −2.2% to 3.2%. Model-based device sizing showed excellent interrater ($\kappa = 0.72$, $P < .0001$) and intrarater ($\kappa = 0.86$, $P < .0001$) agreement. Measurements on models and 3D TEE imaging corresponded well for major (24.2 ± 3.2 vs 24.3 ± 3.2 mm; $r = 0.90$, $P < .0001$; bias = −0.007 mm; limits of agreement, −2.8 to 2.8 mm) and minor (19.5 ± 3.7 vs 19.3 ± 3.6 mm; $r = 0.92$, $P < .0001$; bias = 0.23 mm; limits of agreement, −2.7 to 3.2 mm) ostial diameters and depth (33.8 ± 4.8 vs 33.5 ± 4.7 mm; $r = 0.93$, $P < .0001$; bias = 0.26; limits of agreement, −3.3 to 3.8 mm). Compression and protrusion of the clinically implanted device agreed highly with that of the device implanted in models (18.9 ± 5.0% vs 19.3 ± 5.1%; $r = 0.92$, $P < .0001$; bias = −0.3%; limits of agreement, −4.3% to 3.8%) and protrusion (26.9 ± 11.7% vs 27.1 ± 11.6%; $r = 0.95$, $P < .0001$; bias = −0.2%; limits of agreement, −7.4% to 7.1%).

Anatomic Predictors of Mismatched Sizing

There were no significant differences in age, sex, CHA_2DS_2-VASc score, and comorbidities in patients with implanted device not matching 3D model–predicted size compared with those with matched sizing ($P > .05$ for all). Predictors of mismatch were nonwindsock morphology (odds ratio, 4.7; 95% CI, 1.2–32.2; $P = .027$) and presence of prominent trabeculations at the device landing zone (odds ratio, 7.1; 95% CI, 2.4–26.8; $P = .0003$; Table 3, Figure 2).

DISCUSSION

The present study demonstrates in patients undergoing LAA occlusion that device selection concordant with 3D-printed model–based sizing was associated with improved procedural safety and efficacy. In our initial retrospective cohort, we identified that a difference of one device size in the implanted device (selected by 3D TEE imaging and fluoroscopy) compared with the device selected using the in vitro model optimally separated cases associated with and without adverse outcomes. This definition for device matching was then used in a prospective study in which device sizing was first performed in the in vitro model, before the actual procedure. In prospective patients, we demonstrated that a preprocedural model-based sizing strategy as an adjunct to imaging may lead to superior prediction of outcomes. In our cohort, WATCHMAN devices appropriately sized by 3D model had 100% implantation success, with an average of 1.1 devices used per procedure, relative to 94.9% implantation success with 1.39 devices used per procedure in the global WATCHMAN experience.[3] Otton *et al.*[12] first reported using flexible 3D-printed LAA models for planning occlusion. Several other groups,[16,17] including ours,[11] extended the concept to more complex procedures. Wang *et al.*[18] and Hell *et al.*[19] demonstrated high accuracy (≈ 100%) of printed models in predicting correct device size in two prospective cohorts ($n = 75$ in total). Our study confirms these findings in a larger cohort and, importantly, provides outcome analysis for recommending updates in clinical practice.

Pericardial effusion is one of the most serious complications of the percutaneous LAA occlusion procedure. Root-cause analysis in PROTECT-AF (Watchman Left Atrial Appendage System for Embolic Protection in Patients with AF) identified catheter manipulation within the LAA and device deployment itself as common culprits of serious pericardial effusion.[4] Unretracted barbs of an oversized device can also apply localized stress on the appendage wall, potentially causing perforation.[12] Consistent with PROTECT-AF, most of the procedure-related serious pericardial effusions in our cohort were believably caused by either multiple device deployments as a result of poor sizing or implantation of an oversized device, or both. The effusions noted in our study might have been avoided if 3D modeling had been used for device sizing in the first place, because proper size and fewer deployment attempts would have been more likely. Intriguingly, surgically confirmed LAA perforation was reproduced in one of our cases at almost the same location on the appendage 3D model.

In PROTECT-AF, the incidence of device thrombus was 4.2%, consistent with our cohort.[4] Formation of device thrombus may portend clinical events.[4,5] The predilection site of thrombus[8] suggests that the creation of a cul-de-sac, often as a result of deep device implantation, may act as an anatomic substrate for thrombus formation. We demonstrated that 3D modeling accurately predicts such anatomy and resultant thrombus formation and provides information on the proper device size and position to avoid such complication. Potential sites of residual peridevice leak can also be identified by examining areas of inadequate engagement or gaps. Indeed, peridevice leak appears to be associated with thrombus formation as it is present in all our device thrombus cases. Of note, we observed that device thrombus can form with leaks ≤5 mm; thus, the conventional cutoff accepted to be "safe" to discontinue anticoagulation after WATCHMAN implantation may not be truly safe, highlighting the importance of achieving complete occlusion. Three-dimensional modeling allows more confident device sizing to achieve complete

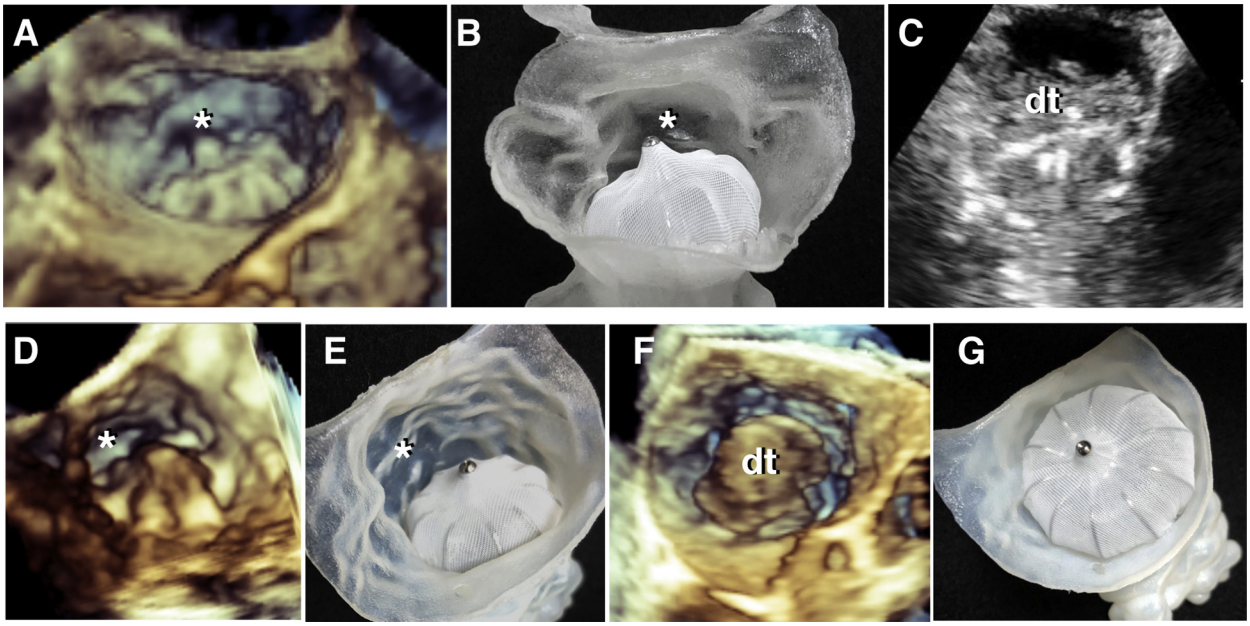

Figure 3 Cases with device thrombus. Case 1: **(A)** Deep implantation of a 33-mm device creates a large cul-de-sac (*asterisks*) beneath the left pulmonary vein ridge as shown on 3D TEE imaging. **(B)** The 3D model accurately predicts the cul-de-sac (*asterisk*) anatomy. **(C)** Formation of device thrombus (dt) in the cul-de-sac 6 months after implantation. Case 2: **(D)** Deep implantation of a 30-mm device creates a deep cul-de-sac (*asterisks*), accurately predicted by **(E)** 3D modeling. **(F)** Formation of a mobile device thrombus (dt) that caused a stroke. **(G)** Three-dimensional modeling shows that a 33-mm device deployed proximally would have obliterated the anatomic nidus for thrombus formation.

Table 5 Device sizing mismatch with 3D model and long-term clinical events in the retrospective cohort

Variable	Model-match group	Model-mismatch group	Hazard ratio (95% CI)	*P*
Composite efficacy endpoint	1/52 (1.9)	4/20 (20.0)	15.6 (4.7–364.7)	.0009
Ischemic stroke/TIA	0/52 (0.0)	2/20 (10.0)	70.5 (2.7–185.4)	.01
CV/unexplained death	1/52 (1.9)	2/20 (10.0)	8.2 (1.2–352.0)	.039
Hemorrhagic stroke	1/52 (1.9)	0/20 (0.0)	0.3 (0.003–25.0)	.57
Systemic embolism	0/52 (0.0)	0/20 (0.0)	NA	NA
All-cause death	5/52 (9.6)	4/20 (20.0)	3.2 (0.9–23.9)	.066
Major bleed (intracranial)	1/52 (1.9)	0/52 (0.0)	0.31 (0.001–84.3)	.68

CV, Cardiovascular; *NA*, not applicable; *TIA*, transient ischemic attack.
Data are expressed as number/total (percentage).

seal in LAA occlusion that could translate into better stroke-preventive efficacy of the procedure.

Although the digital "blueprints" for 3D printing are derived from the 3D TEE image data set, the physical models provide unique information on device-tissue interactions not available from the native imaging data. It was not the measurements but rather the ability to test devices in the in vitro setting to identify potential problems with certain devices that provided important information highly relevant to implantation outcomes. For instance, occluding an LAA with branching lobes may require special techniques and device sizing methods that may be different from conventional scale on the basis of TEE measurements.[11] Computational simulation may provide similar information but demands complex finite element analysis with boundary assumptions. Three-dimensional printing would therefore be a more practical and potentially more accurate approach. Although the current costs of the printer and associated software license are high, the material cost of 3D printing per model was only approximately $15 to $30, and the turnaround time was approximately 4 to 6 hours (full details are provided in Supplemental Table 1 in the Appendix, available at www.onlinejase.com). The additional upfront cost and time are likely to be offset by reduced procedural time and complications. In our experience, preprocedural 3D printing fits seamlessly in our routine workflow and does not require patients to undergo any additional procedures.

Limitations

The current study had several limitations. First, this investigation was a nonrandomized study. It was, nevertheless, by far the largest series of 3D TEE 3D printing in LAA occlusion showing a statistically significant outcome benefit associated with 3D printing adjusted for potential confounders. The comparison between 3D modeling in the

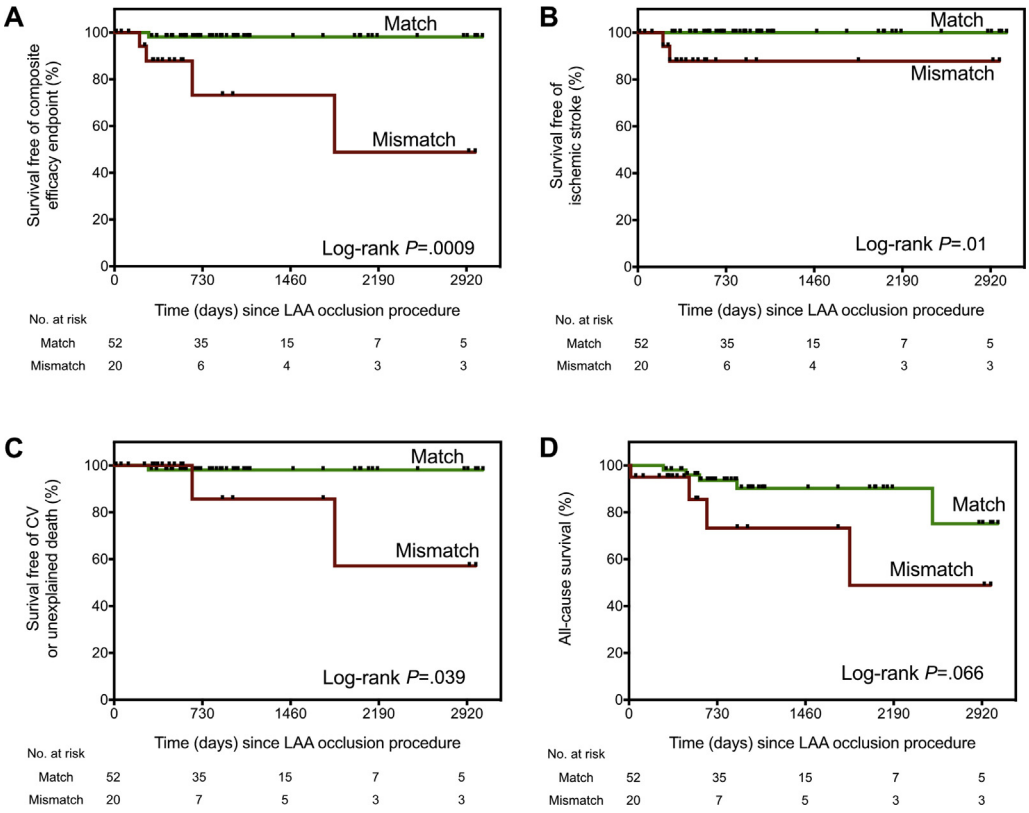

Figure 4 Kaplan-Meier curves of patients with model-match and model-mismatch sizing in the retrospective cohort. Kaplan-Meier curves for long-term efficacy end points according to whether the implanted device matches the 3D modeling prediction. The model-mismatch group had a significantly ($P < .05$) higher cumulative incidence of **(A)** composite efficacy end points (all strokes, cardiovascular (CV) or unexplained death, or systemic embolism), **(B)** ischemic stroke, and **(C)** cardiovascular or unexplained death. There was no statistically significant difference in all-cause death between the two groups **(D)**.

Table 6 Comparison of procedural events and follow-up device problems between retrospective and prospective cohorts

Variable	Retrospective cohort	Prospective cohort	*P*
Procedure time (min), median (range)	60 (25–150)	41 (30–55)	<.0001
Implant success	67/72 (93.1)	32/32 (100.0)	.32
Device used per procedure, mean (range)	1.3 (1–4)	1.1 (1–2)	.046
Composite procedural major safety events within 7 days	6/72 (8.3)	0/32 (0.0)	.17
Serious pericardial effusion	5/72 (6.9)	0/32 (0.0)	.32
Air embolism	1/72 (1.4)	0/32 (0.0)	≥.999
Device complications/problems on follow-up TEE imaging			
Device thrombus	4/64 (6.3)	0/32 (0.0)	.30
Peridevice leak			.015
None	44/64 (64.1)	31/32 (96.9)	
<1 mm	1/64 (1.6)	0/32 (0.0)	
1–3 mm	17/64 (25.6)	1/32 (3.1)	
>3–5 mm	4/64 (6.3)	0/32 (0.0)	
>5 mm	1/64 (1.6)	0/32 (0.0)	

Data expressed as number/total (percentage) except as indicated.

prospective cohort and standard imaging in the historical cohort provides promising data regarding the advantage of 3D modeling. The relatively small number of events may present difficulty for adjustment for predictors of outcome. Larger randomized studies are warranted to confirm the value of model-based sizing for predicting outcome.

Second, not all adverse outcomes can be attributed to poor device sizing. Pericardial effusion can be caused, for instance, by injury from

guidewires in the left atrium or transseptal puncture.[4] Device thrombus formation depends on the interplay of device-specific and patient-specific factors.[5] Three-dimensional modeling in our cohort did not predict (and would not be expected to predict) an air embolism, tamponade possibly caused by injury of a non-LAA structures, a late hemorrhagic stroke, and device thrombus in a patient with high CHA_2DS_2-VASc score who was not anticoagulated after implantation.

Third, volume depletion can underestimate LAA size but is rectifiable by preimaging rehydration, and this issue affects computed tomography as well.[19]

Finally, limited by the field of view of 3D TEE imaging, the interatrial septum was not modeled in this study. The angle of approach of the device deployment system is partially dependent on the spatial relationship between the transseptal puncture site and the LAA and may have an impact upon how a device "sits" in the LAA during and after deployment. Nevertheless, the location of transseptal puncture and the angle of approach were standardized during the clinical procedures. The angle of approach was accounted for by maintaining catheter coaxiality with the LAA in the in vitro setting resembling clinical implantation.

CONCLUSION

By combining the technologies of 3D TEE imaging and 3D printing with tissue-mimicking materials, we demonstrated that patient-specific 3D modeling offers incremental outcome-relevant information for LAA occlusion. Application of 3D printing may directly affect our ability to select appropriate patients and devices for LAA occlusion, anticipate procedural complexity, and improve intraprocedural performance and safety, especially in challenging anatomy. Whether a personalized approach with 3D modeling for LAA occlusion could improve the long-term efficacy and outcome of the procedure must be confirmed by head-to-head comparison between 3D modeling and standard imaging in prospective randomized trials.

SUPPLEMENTARY DATA

Supplementary data to this article can be found online at https://doi.org/10.1016/j.echo.2019.02.003.

REFERENCES

1. Holmes DR, Reddy VY, Turi ZG, Doshi SK, Sievert H, Buchbinder M, et al. Percutaneous closure of the left atrial appendage versus warfarin therapy for prevention of stroke in patients with atrial fibrillation: a randomized non-inferiority trial. Lancet 2009;374:534-42.
2. Holmes DR Jr., Kar S, Price MJ, Whisenant B, Sievert H, Doshi SK, et al. Prospective randomized evaluation of the WATCHMAN left atrial appendage closure device in patients with atrial fibrillation versus long-term warfarin therapy: the PREVAIL trial. J Am Coll Cardiol 2014;64:1-12.
3. Reddy VY, Gibson DN, Kar S, O'Neill W, Doshi SK, Horton RP, et al. Post-approval U.S. Experience with left atrial appendage closure for stroke prevention in atrial fibrillation. J Am Coll Cardiol 2017;69:253-61.
4. Reddy VY, Holmes D, Doshi SK, Neuzil P, Kar S. Safety of percutaneous left atrial appendage closure: results from the WATCHMAN left atrial appendage system for embolic protection in patients with AF (PROTECT AF) clinical trial and the continued access Registry. Circulation 2011;123:417-24.
5. Main ML, Fan D, Reddy VY, Holmes DR, Gordon NT, Coggins TR, et al. Assessment of device-related thrombus and associated clinical outcomes with the WATCHMAN left atrial appendage closure device for embolic protection in patients with atrial fibrillation (from the PROTECT-AF Trial). Am J Cardiol 2016;117:1127-34.
6. Veinot JP, Harrity PJ, Gentile F, Khandheria BK, Bailey KR, Eickholt JT, et al. Anatomy of the normal left atrial appendage: a quantitative study of age-related changes in 500 autopsy hearts: implications for echocardiographic examination. Circulation 1997;96:3112-5.
7. So CY, Cheung GSH, Chan AKY, Lee APW, Lam YY. A call for standardization in left atrial appendage occlusion. J Am Coll Cardiol 2018;72:472-3.
8. Wunderlich NC, Beigel R, Swaans MJ, Ho SY, Siegel RJ. Percutaneous interventions for left atrial appendage exclusion: options, assessment, and imaging using 2D and 3D echocardiography. JACC Cardiovasc Imaging 2015;8:472-88.
9. Saw J, Lempereur M. Percutaneous left atrial appendage closure: procedural techniques and outcomes. JACC Cardiovasc Interv 2014;7:1205-20.
10. Giannopoulos AA, Mitsouras D, Yoo SJ, Liu PP, Chatzizisis YS, Rybicki FJ. Applications of 3D printing in cardiovascular diseases. Nat Rev Cardiol 2016;13:701-18.
11. Fan Y, Kwok KW, Zhang Y, Cheung GS, Chan AK, Lee AP. Three-dimensional printing for planning occlusion procedure for a double-lobed left atrial appendage. Circ Cardiovasc Interv 2016;9:e003561.
12. Otton JM, Spina R, Sulas R, Subbiah RN, Jacobs N, Muller DW, et al. Left atrial appendage closure guided by personalized 3D-printed cardiac reconstruction. JACC Cardiovasc Interv 2015;8:1004-6.
13. Yu CM, Khattab AA, Bertog SC, Lee APW, Kwong JSW, Sievert H, et al. Mechanical antithrombotic intervention by LAA occlusion in atrial fibrillation. Nat Rev Cardiol 2013;10:708-23.
14. Su P, McCarthy KP, Ho SY. Occluding the left atrial appendage: anatomical considerations. Heart 2008;94:1166-70.
15. Spencer RJ, DeJong P, Fahmy P, Lempereur M, Tsang MYC, Gin KG, et al. Changes in left atrial appendage dimensions following volume loading during percutaneous left atrial appendage closure. JACC Cardiovasc Interv 2015;8:1935-41.
16. Liu P, Liu R, Zhang Y, Liu Y, Tang X, Cheng Y. The value of 3D printing models of left atrial appendage using real-time 3D transesophageal echocardiographic data in left atrial appendage occlusion: applications toward an era of truly personalized medicine. Cardiology 2016;135:255-61.
17. Pellegrino PL, Fassini G, DI Biase M, Tondo C. Left atrial appendage closure guided by 3D printed cardiac reconstruction: emerging directions and future trends. J Cardiovasc Electrophysiol 2016;27:768-71.
18. Wang DD, Eng M, Kupsky D, Myers E, Forbes M, Rahman M, et al. Application of 3-dimensional computed tomographic image guidance to WATCHMAN implantation and impact on early operator learning curve: single-center experience. JACC Cardiovasc Interv 2016;9:2329-40.
19. Hell MM, Achenbach S, Yoo IS, Franke J, Blachutzik F, Roether J, et al. 3D printing for sizing left atrial appendage closure device: head-to-head comparison with computed tomography and transoesophageal echocardiography. EuroIntervention 2017;13:1234-41.

APPENDIX

ROC Analysis

For the retrospective cohort, an ROC curve was generated using adverse outcome as the principle end point (state variable). Adverse outcome was defined as the occurrence of any of the following: implantation failure, any procedural safety event within 7 days, significant peridevice leak (>5 mm), device thrombus, and composite efficacy events including all stroke, systemic embolism, and cardiovascular or unexplained death. Area under the curve was evaluated for 3D model device sizing, using Δ ([diameter of 3D model–suggested device) minus [diameter of device implanted]) as the independent variable. A specific upper cutoff was defined using the ROC curve, on the basis of the Δ value corresponding to the highest sum of sensitivity and specificity for discriminating adverse and nonadverse outcomes. The ROC curve analysis showed that 3D model device testing had good discriminatory value for adverse outcomes, with area under the curve of 0.81 ($P = .0002$; Supplemental Figure 1). An upper cutoff of 3 mm had sensitivity of 73% and specificity of 84%.

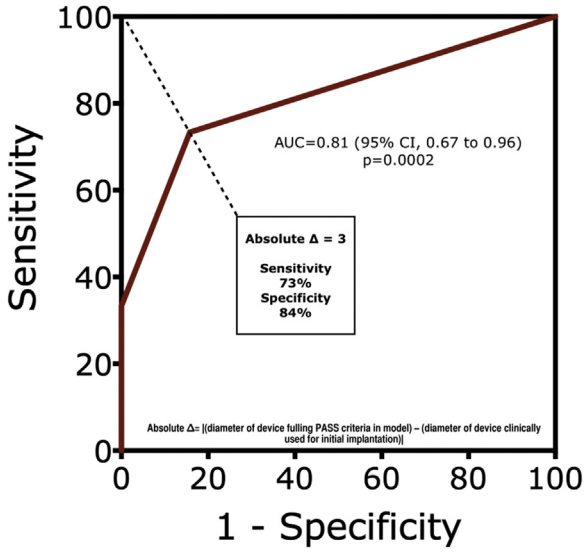

Supplemental Figure 1 ROC curve for discriminating adverse and nonadverse outcomes. *AUC*, Area under the curve.

Time and Cost of 3D Printing

Three-dimensional TEE image postprocessing took 30 min per case. Printing one batch of seven models took 4 hours. Postprinting removal of support materials took 15 min per model. The cost of materials for 3D printing per model is approximately $15 to $30 (Supplemental Table 1). An alternative to purchasing the printer and materials is to use an external service, which would cost about $80 to $100 per model in our region. Demonstration LAA occluder devices used in in vitro testing are reusable and would not add to the cost of consumables.

Supplemental Table 1 Estimated cost of 3D printing of LAA models

Items	Estimated cost (US dollars)
Materials for 3D printing	$15 to $30
Installation of 3D printer	$120,000
Software license	$50,000
External printing service	$80 to $100 per model
LAA occluder device used for in vitro 3D model testing	$7,000 per occluder (reusable)